Numerical Study on Flow and Thermal Characteristics in Flow Channel of Transpired Solar Collector

Qian Gao, Dengjia Wang, Yanfeng Liu, Yingying Wang, Yuan Liu and Jiaping Liu

Abstract At present, it is urgent to improve indoor air quality while improving indoor thermal environment in winter, which is the ultimate goal in the field of architectural environment. The transpired solar collector (TSC), a solar energy integration technology in buildings, was proposed, which usually consists of a heat collecting plate with infiltration holes, an air layer, an insulation wall, an air outlet, and other auxiliary devices. In this paper, the physical models of transpired solar collector were developed, and the model is simplified to facilitate the simulation calculation and be verified through experiments to improve the reliability of the simulation results. By using numerical simulation to carry on the comprehensive and multi-case study of transpired solar collector, such as solar radiation intensities, fan suction speeds, infiltration hole non-uniform distribution up and down, and infiltration hole diameters for flow and thermal characteristics in flow channel of transpired solar collector were analyzed. The results show that the height ratio has the most obvious influence on the flow and thermal characteristics in the air layer compared with other key design and

Q. Gao · D. Wang (✉) · Y. Liu · Y. Wang · Y. Liu · J. Liu
State Key Laboratory of Green Building in Western China, Xi'an University of Architecture and Technology, Xi'an 710000, China

School of Building Services Science and Engineering, Xi'an University of Architecture and Technology, Xi'an 710000, China
e-mail: 18309204225@163.com

D. Wang
e-mail: wangdengjia@xauat.edu.cn

Y. Liu
e-mail: lyfxjd@163.com

Y. Wang
e-mail: 1274296191@qq.com

Y. Liu
e-mail: 1427368868@qq.com

J. Liu
e-mail: liujiaping@xauat.edu.cn

Z. Wang et al. (eds.), *Proceedings of the 11th International Symposium on Heating, Ventilation and Air Conditioning (ISHVAC 2019)*, Environmental Science and Engineering, https://doi.org/10.1007/978-981-13-9528-4_36

operation parameters. The results can lay a foundation for the large-scale processing and application of transpired solar collector, which is instructive.

Keywords Transpired solar collectors · Flow channel · Flow and thermal characteristics · Experiment · Numerical simulation

1 Introduction

Building energy consumption and environmental problems are increasingly serious [1], and the search for renewable energy such as solar energy to alleviate this problem has become a hot spot. At present, among the various utilization methods of solar energy, the passive solar technology [2], such as direct-gain window, attached sunroom, and solar wall, is the most simple and easy to operate with low technical cost. Among them, solar wall is favored by many scholars for its advantages of better architectural integration and strong plasticity.

At present, there are many studies on the solar wall with heat collecting and heat storage, and the most representative one is the Trombe wall designed by French scientist Felix Trombe and built in Odysseus in 1967 [3–5]. The research on this kind of solar wall mainly focuses on the types of Venetian blind solar wall [6, 7], heat pipe-type solar wall [8], and lattice-type solar wall [9]. The results show that these solar walls can effectively improve indoor temperature and reduce heating load in winter. However, these wall structures are of internal circulation type, and it is difficult to take into account the improvement of indoor air quality in winter.

Therefore, transpired solar collectors (TSCs) are proposed, including the heat collecting system and the air flow conveying system. The operating principle of the TSC is shown in Fig. 1. The heat collecting system includes infiltration heat collecting plate, air layer and infiltration holes, and other auxiliary devices. The air in the air layer absorbs the radiant heat of the heat collecting plate through thermal convection, so as to preheat the fresh air. Europe, the USA, and some countries have made some attempt in the practical application, such as Conversal company in Canada and the UK at Cardiff university, etc., and achieved good effect [10, 11], Afterward, Dymond and Kutscher set the porous plate as the boundary condition of continuous fluid, carried out overall CFD simulation analysis on the solar wall, and obtained the temperature and pressure of the air at the outlet of the air layer [12]. Decker et al. studied the heat exchange efficiency with different hole shapes based on Kutscher's study [13]. However, the research on TSC above mainly focuses on the uniform distribution of infiltration holes, and seldom considers the short-circuit problem caused by the non-uniform distribution of infiltration holes under the action of thermal pressure and wind pressure. In addition, since TSC air layer flow mainly depends on the vertical thermal pressure and wind pressure, it is necessary to understand the influence of TSC key structural design parameters and operating parameters on the air layer temperature field and velocity field.

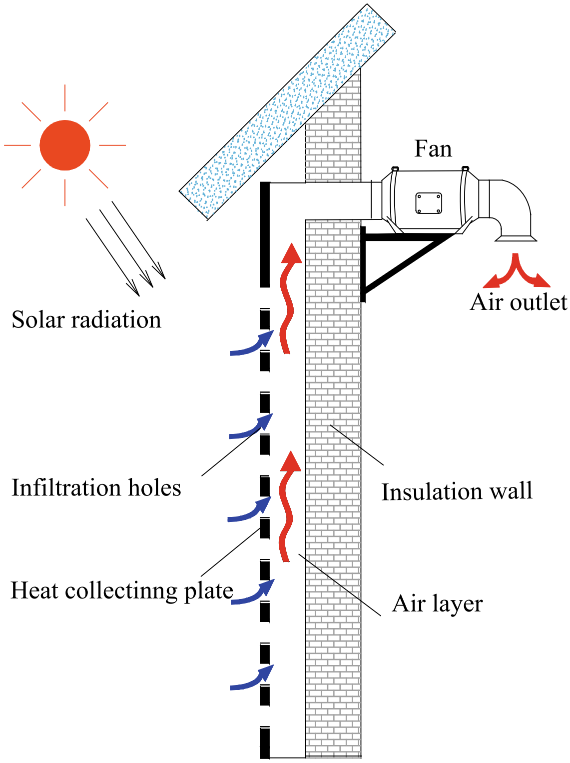

Fig. 1 Operating principle of TSC

In this paper, the flow and thermal characteristics in the flow channel of the TSC are analyzed through numerical simulation under the conditions of different solar radiation intensities, suction speeds, and ratios of the height of the infiltration hole to the height of the heat collecting plate. The effect laws of various parameters on the thermal and flow characteristics in flow channel of TSC were obtained. The conclusion can provide a reference for the design of TSC.

2 Methods

A high-resolution computational domain has been created to reproduce the physical TSC system, so as to capture the multi-scale fluid flow behavior which establishes over the perforated plate and within the perforations. The structure, geometric shape, and boundary condition details of CFD model are shown in Fig. 2.

The experiment was set up in State Key Laboratory of Green Building in Western China. Experimental data from above experimental tests were used for model validation as well as boundary and initial conditions for the simulation; the details of verification conditions are shown in Table 1.

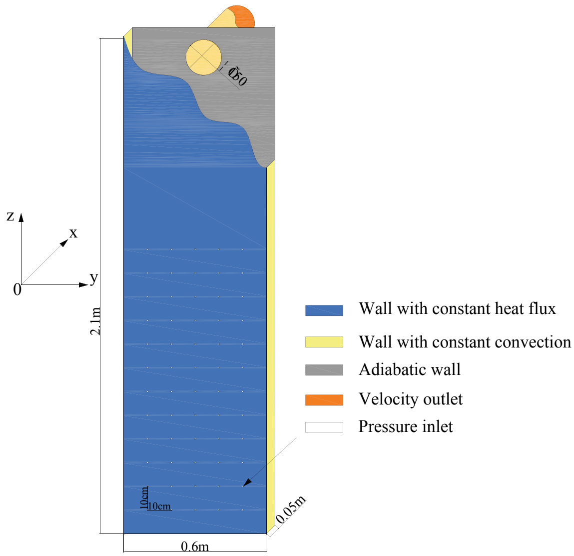

Fig. 2 Computational domain and boundary details

Table 1 Details of the cases used for validation

Case number	Ambient air temperature (°C)	Solar radiation intensities I (W/m^2)	Fan suction speeds v_s (m/s)	Hole diameter D (mm)	Height ratio H^a
1	24.0	700	0.525	4	0.6
2	25.0	600	0.525	4	0.6
3	22.4	600	0.525	2	0.6
4	20.1	700	0.525	2	0.3
5	22.7	600	0.525	2	0.3
6	24.2	500	0.525	2	0.3
7	16.3	600	0.725	4	0.3
8	22	700	0.525	2	0.9
9	23.2	600	0.525	2	0.9
10	22.1	700	0.525	6	0.6

[a] H means ratio of the height of the infiltration hole to the height of the heat collecting plate

The calculation model uses the standard k-ε two-equation model, introduces the Boussineq hypothesis, and turns on the DO radiation model. In solution methods, the spatial discretization method of pressure is PRESTIO! The momentum and energy equations adopt the second-order windward scheme. The remaining options are in a first-order upwind format. SIMPLEC algorithm is adopted for iterative solution. The simulation conditions were shown in Table 2.

Table 2 Infiltration hole diameters, height ratios, fan suction speeds, and solar radiation intensities for various operating conditions

Infiltration hole diameters D (mm)	2	4	6	–
Height ratios H^*	0.3	0.6	0.9	–
Fan suction speeds v_s (m/s)	0	0.525	0.725	0.925
Solar radiation intensities I (W/m^2)	500	600	700	–

* representing the ratio of the height of the hole rows on the heat collecting plate to the overall height of the heat collecting plate, which is a dimensionless quantity

3 Results

3.1 Model Validation

A comprehensive and operable TSC experimental platform was built indoors to verify the CFD model. The conditions with certain real reliability were selected for validation, as shown in Table 1. The temperature of heat collecting plate, air outlet, and air layer were verified respectively. Figure 3 is the comparison between the numerical simulation results and the experimental test results. The results show that the relative error, which are outlet temperature, heat collecting plate temperature and air layer temperature between the numerical calculation and the experimental results is within 10%. For the convenience of calculation, it is believed that there is

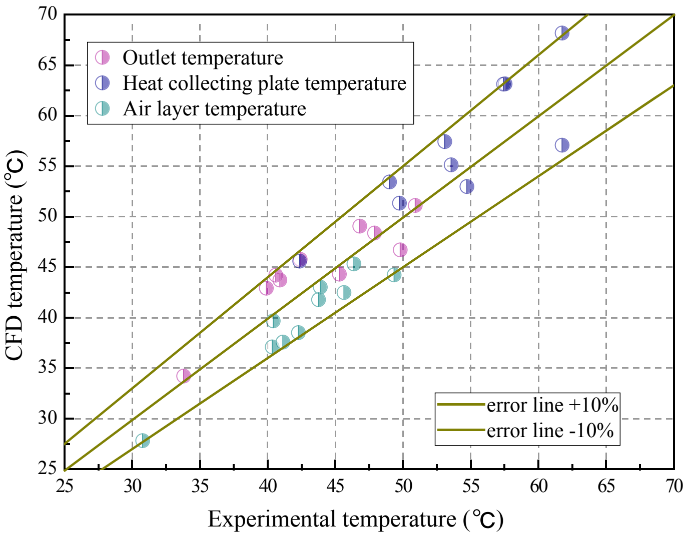

Fig. 3 Comparison between CFD simulation and experimental data

a certain difference between the calculated results and the measured results. Due to the constant ambient temperature, the error is not more than 15%.

3.2 The Velocity Distribution of Flow Channel Under Different Parameters

Under the suction action of the fan, because the diameter of the infiltration hole is very small and the size of the outlet is relatively large, according to the conservation of mass, the air speed at the infiltration hole increases sharply. As shown in Fig. 4a, with the increase of the ratio of opening height, from 0.3 to 0.9, the air speed around the infiltration hole gradually decreases. Along the direction of the flow channel height, the velocity in the flow channel will gradually decrease and eventually reach the basic stability. The solar radiation intensity has little influence on the velocity inside the air layer, as shown in Fig. 4b. The solar radiation intensity increases from 500 to 700 w/m^2, and the velocity curves in the flow channel basically coincide, fluctuating at 0.03 m/s. The velocity fluctuation from the infiltration hole area to

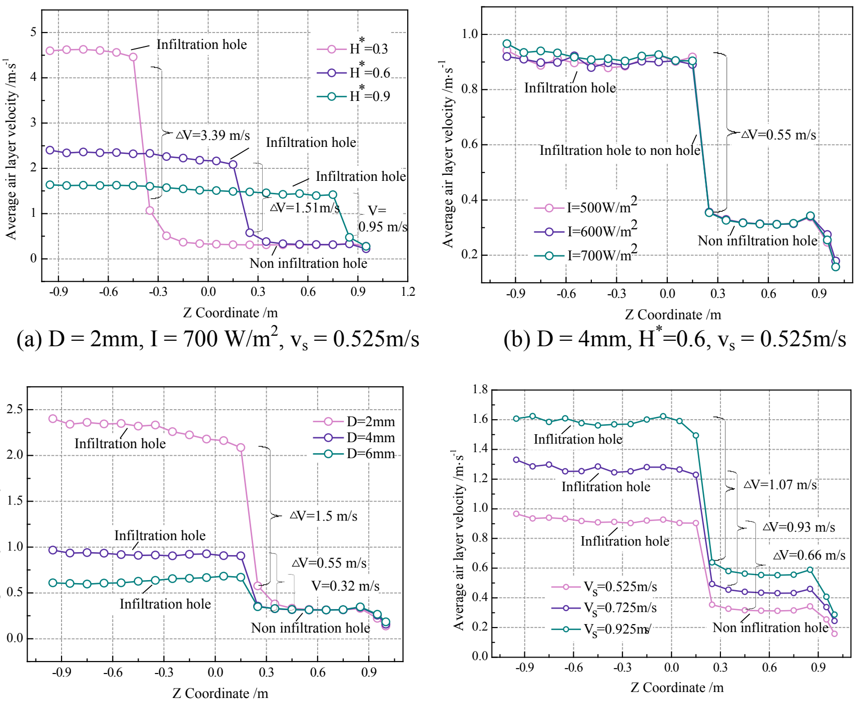

(a) D = 2mm, I = 700 W/m^2, v_s = 0.525m/s (b) D = 4mm, H*=0.6, v_s = 0.525m/s

(c) I =700 W/m^2, H*=0.6, v_s = 0.525m/s (d) I =700 W/m^2, H*=0.6, D = 4mm

Fig. 4 Air layer velocity trend along the height of the flow channel the non-infiltration hole area is 0.55 m/s. Near the top outlet, the velocity decreases sharply due to the increase in the air circulation area.

Figure 4c shows the influence of different infiltration hole diameters on the flow characteristics in the flow channel. If the infiltration hole diameter increases, the overall velocity in the air layer flow channel will decrease. The infiltration hole diameter increased from 2 to 4 mm and then to 6 mm, and the velocity around the infiltration hole decreased by about 1.36 and 0.29 m/s, respectively. In the flow channel in the non-infiltration hole area, the velocity drops sharply and tends to be flat, around 0.32 m/s. The suction velocity has a great influence on the velocity in the air layer flow channel, as shown in Fig. 4d. When the suction speed is changed, the change trend of velocity along the flow channel direction is basically the same. The suction speed increased from 0.525 to 0.725 m/s and then to 0.925 m/s. The velocity near the infiltration hole increased by about 0.35 m/s and 0.31 m/s, respectively.

3.3 The Temperature Distribution of Flow Channel Under Different Parameters

In comparison with Fig. 4, the temperature distribution and velocity distribution have basically opposite trends. Under different height ratios, the temperature distribution of the air layer flow channel is shown in Fig. 5a. As the height ratio increases, the temperature distribution inside the flow channel is more uniform, and the range of the air flow disturbance is larger, so that the heat exchange between the air and the heat collecting plate is more sufficient, and the increase of the height ratio causes the temperature of the whole field to be significantly improved. H^* increases from 0.3 to 0.9; the temperature of the flow channel increases by about 16 °C and increases about 8 °C near the air outlet.

The increase of solar radiation intensity causes the heat collecting plate to absorb more heat, so that the influence on the temperature distribution in the flow channel is more obvious. As shown in Fig. 5b, as the solar radiation intensity increases, the temperature of the whole flow channel increases. The temperature remained substantially constant at the opening hole because the outdoor cold air continuously entered at the opening hole so that there was no significant increase in temperature along the height of the flow channel. For every 100 W/m^2 increase in solar radiation intensity, the temperature in the flow channel at the same position increases by 2.7 °C.

As can be seen from Fig. 5, the air temperature in the flow channel corresponding to the absence of a hole in the heat collecting plate increases rapidly along the direction of the runner. At the highest position, compared to 2 mm infiltration hole diameter and 6 mm infiltration hole, temperature rises around 8 °C. The fan suction speed can change the wind pressure inside the entire flow channel, which has a greater impact on the temperature field distribution. As shown in Fig. 5d, increase the suction speed overall temperature decreased obviously in the flow channel, the air speed increased from 0.525 to 0.725 m/s, 4.3 °C temperature decrease; Increased from 0.725 to

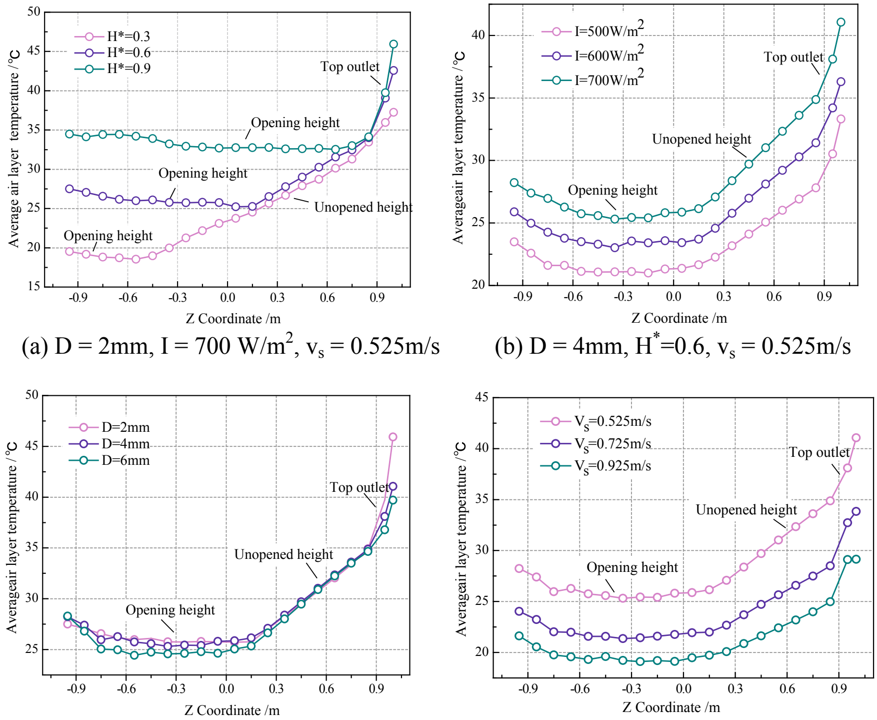

(a) D = 2mm, I = 700 W/m^2, v_s = 0.525m/s (b) D = 4mm, H*=0.6, v_s = 0.525m/s

(c) I =700 W/m^2, H*=0.6, v_s = 0.525m/s (d) I =700 W/m^2, H*=0.6, D = 4mm

Fig. 5 Air layer temperature trend along the height of the flow channel

0.925 m/s, 2.5 °C temperature decrease. So, as the suction speed increases, the rate of temperature decrease also decreases.

4 Conclusions

A high-resolution, three-dimensional, steady, CFD approach has been developed to model TSC system. The following can be concluded from the investigations carried out thus far:

(1) The velocity distribution is contrary to the temperature distribution trend in the air layer flow channel. In order to meet the demand of necessary fresh air volume, the suction speed should be reduced as far as possible to meet the demand of fresh air preheating.
(2) The solar radiation intensity has the least impact on the flow characteristics in the flow channel, and the infiltration hole diameter has the least impact on the thermal characteristics in the flow channel.

(3) Compared with other key parameters, the height ratio has great influence on both TSC flow and thermal characteristics.

Acknowledgements This study was supported by the National Key Research and Development Program (No. 2016YFC0700400); the National Natural Science Foundation of China (No. 51678468); and the Shaanxi Youth Science and Technology Nova Project (No. 2017KJXX-22).

References

1. Study of urban sewage heat energy utilization and its application, Jilin University, Jilin
2. Liu, Y., Li, Z.: Research on passive solar energy utilization building technology. Urban Constr. Theory Res. Electron. Ed. **5**(31), 2167–2168 (2015)
3. Chen, Q.Z.: Application Research of Passive Solar Building with Phase Change Wallboard in Shenyang Area. Chongqing University, Chongqing (2010)
4. Torcellini, P., Pless, S.: Trombe Walls in low-energy buildings: practical experiences, Preprint (2004)
5. Safer, N., Woloszyn, M., Roux, J.J.: Three-dimensional simulation with a CFD tool of the airflow phenomena in single floor double-skin facade equipped with a venetian blind. Sol. Energy **79**(2), 193–203 (2005)
6. He, W., Wang, C.C., Ji, J.: Study on the effect of Trombe wall with venetian blind structure on indoor temperature in different blade angle. J. Sol. Energy **3**(37), 673–677 (2016)
7. Chen, C., Liu, Y.F., Wang, D.J., et al.: The optimization and adaptation analysis on the Insulation structure of the Trombe wall. J. Sol. Energy **37**(11), 2889–2895 (2016)
8. Zhang, Z.J., Xiang, S.C., Zhang, Y.F., et al.: A new type of hybrid magnetic semiconductor based upon polymeric iodoplumbate and metal-organic complexes as templates. Inorg. Chem. **45**(5), 1972–1977 (2006)
9. Wang, W.L., Tian, Z., Ding, Y.: Investigation on the influencing factors of energy consumption and thermal comfort for a passive solar house with water thermal storage wall. Energy Build. **64**(5), 218–223 (2013)
10. Conserval Engineering Inc, 2010. Solar-Wall SW150/SW250 Profile[EB/OL]. http://solarwall.com/en/products/solar-wall-airheating/architects-and-engineers
11. Saxena, A., Varun, El-Sebaii, A.A.: A thermodynamic review of solar air heaters. Renew. Sustain. Energy Rev. **43**, 863–890 (2015)
12. Dymond, C., Kutscher, C.: A computer design model for transpired solar collector systems. In: Proceedings of the ASME/JSME/JSES International Solar Energy Conference, vol. 02, pp. 1165–1174. American Society of Mechanical Engineers, New York (1995)
13. Decker, G.W.E.V., Hollands, K.G.T., Brunger, A.P.: Heat-exchange relations for unglazed transpired solar collectors with circular holes on a square or triangular pitch. Sol. Energy **71**(1), 33–45 (2001)